We are IntechOpen, the world's leading publisher of Open Access books Built by scientists, for scientists

6,900
Open access books available

185,000
International authors and editors

200M
Downloads

154
Countries delivered to

Our authors are among the

TOP 1%
most cited scientists

12.2%
Contributors from top 500 universities

BOOK CITATION INDEX
CLARIVATE ANALYTICS
INDEXED

WEB OF SCIENCE™

Selection of our books indexed in the Book Citation Index
in Web of Science™ Core Collection (BKCI)

Interested in publishing with us?
Contact book.department@intechopen.com

Hybrid Nature Properties of Tl$_{10-x}$ATe$_6$ (A = Pb and Sn) Used as Batteries in Chalcogenide System

Waqas Muhammad Khan and Wiqar Hussain Shah

Abstract

In future, the most common batteries will be the thallium. As there is many types of batteries but the thallium batteries are better from them. In here, we have made the compound which is more positive work than the other batteries. The different elements are doping in the tellurium telluride to determine the different properties like electrical and thermal properties of nanoparticles. The chalcogenide nanoparticles can be characteristics by the doping of the different metals which are like the holes. We present the effects of Pb and Sn doping on the electrical and thermoelectric properties of Tellurium Telluride Tl$_{10-x}$Pb$_x$Te$_6$ and Tl$_{10-x}$Sn$_x$Te$_6$ (x = 1.00, 1.25, 1.50, 1.75, 2.00) respectively, which were prepared by solid state reactions in an evacuated sealed silica tubes. Structurally, all these compounds were found to be phase pure as confirmed by the x-rays diffractometery (XRD) and energy dispersive X-ray spectroscopy (EDS) analysis. The thermo-power or Seebeck co-efficient (*S*) was measured for all these compounds which show that *S* increases with increasing temperature from 295 to 550 K. The Seebeck coefficient is positive for the whole temperature range, showing p-type semiconductor characteristics. Similarly the electrical conductivity (σ) and the power factors have also complex behavior with *Pb and Sn* concentrations. The power factor (PF = S^{2}σ) observed for Tl$_{10-x}$Pb$_x$Te$_6$ and Tl$_{10-x}$Sn$_x$Te$_6$ compounds are increases with increase in the whole temperature range (290 K–550 K) studied here. Telluride's are narrow band-gap semiconductors, with all elements in common oxidation states, according to (Tl$^+$)9(Pb^{3+})(Te^{2-})6 and (Tl$^+$)9(Sn^{3+})(Te^{2-})6. Phases range were investigated and determined with different concentration of *Pb and Sn* with consequents effects on electrical and thermal properties.

Keywords: Pb and Sn doping, Seebeck coefficient, electrical conductivity, power factor

1. Introduction

The thermo-electro-materials are now used as the renewable energy. It is used as the place of the coal, water tides, solar cells etc. The thermo electro-materials have more efficiency and reliable. Thermoelectric is one of the most important approaches in the solid state physics which can be converted the heat energy in the electrical energy, help to increase the efficiency, effectiveness and competency. It's importance is increase since last twenty years when the ease of use of fossil fuel is decrease. So there are different thermoelectric materials are used for the different temperatures

from 10 K to the 1000 K which are used in the different applications for the cooling and heating [1–5]. Tellurium telluride is one important compound of the thermoelectric material which is studied, modified and increases the efficiency for the more and more applications for generation of power [1] and solar cells [2]. Tellurium telluride is a basically alloy that is used for the increases the energy conversion efficiency at the any temperature of the heating and cooling in the electrical circuit [3–7].

The figure of merit is

$$ZT = \frac{S^2 \sigma T}{k} \tag{1}$$

Where is σ is the electrical conductivity, k is the thermal conductivity, S is the see-beck coefficient, and T is the absolute temperature which is determined the efficiency of the thermo electric materials applications [8]. The power factors can be determined the electrical and thermal properties. The power factor can be defined as $S^2\sigma$. It can be help the determination of the charge carrier's concentration, from the doping concentration charges and lay down the free electrons in the system of chalcogenides.

We have investigated the chalcogenide with different materials (lead, tin, bismuth etc.) doped in the tellium tellurides. They have complex composition and structure on the basis of the electronic configurations. These compositions help to increases their properties like thermal, electrical, optical etc. of the thermo-electrical materials. There are many challenges of complex composition to high their electrical conductivity, high see-beck coefficient and low thermal conductivity. Due to this, they can controlled the electronic structures of the system i.e. band gap, shapes and degenerated level which is near the Fermi level, concentration of electrons and charge carriers scattered depend on them [7, 8].

Here is defined the basic chemical properties and are related by physical properties of different i.e. S, Se, and Te which are compared in **Figure 1**. Better rate performance and higher utilization rate of active materials can be realized in Te-based batteries. It is worth noting that Te delivers lower gravimetric capacity ($419\,\mathrm{mAh\,g^{-1}}$) than S ($1672\,\mathrm{mAh\,g^{-1}}$) and Se ($675\,\mathrm{mAh\,g^{-1}}$); this disadvantage can
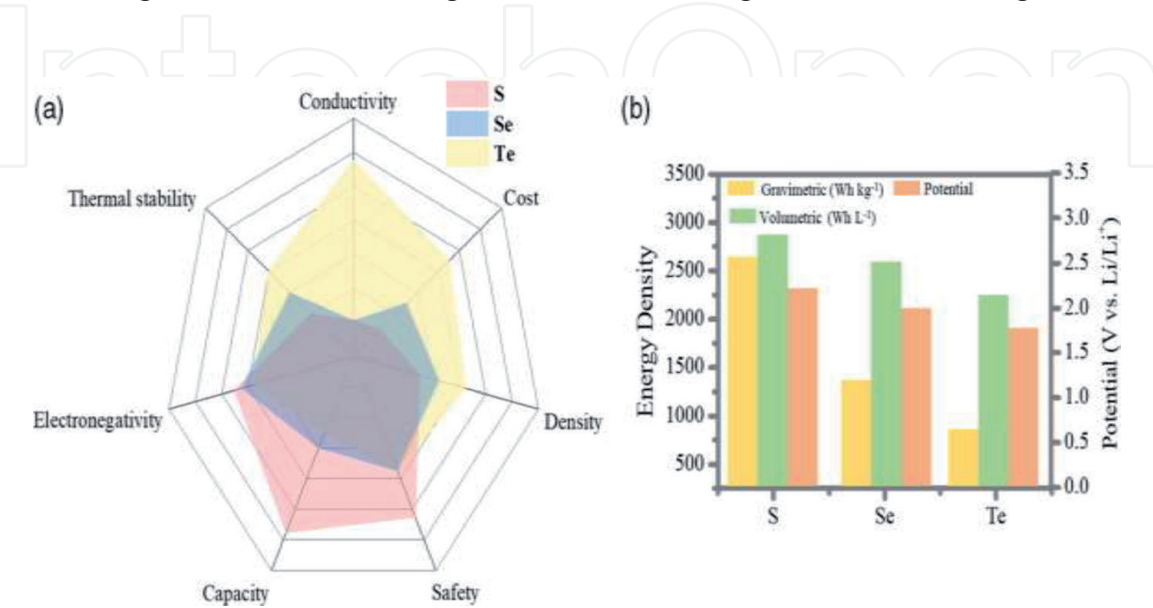

Figure 1.
(a) Comparison of S, Se, and Te based on various properties. (b) Energy density and plateau voltage of Li-S, Li-Se, and Li-Te batteries.
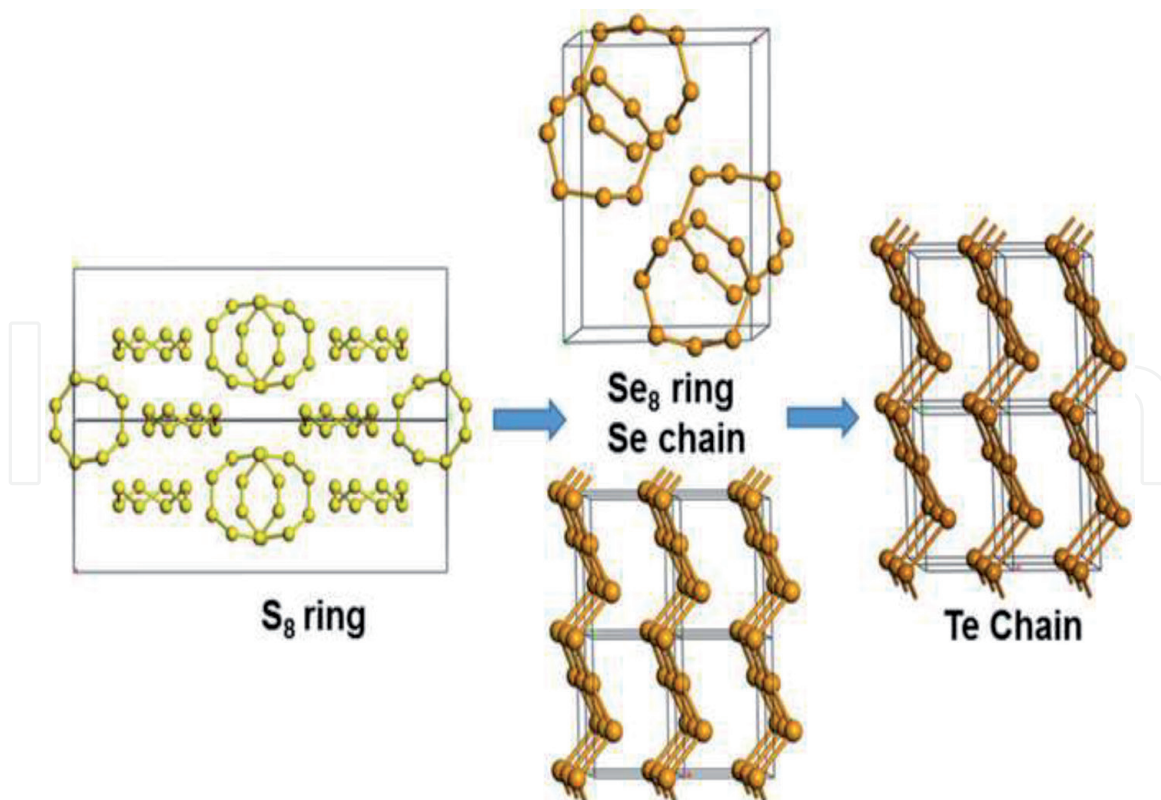
Figure 2.
Crystal structure transformations of S, Se, and Te. S crystal is constructed by S8 rings. Se crystals contain either Se$_8$ rings or Se chains. Te crystal only has chain-like structures. The difference in structure indicates that three congener elements exhibit distinctive structure changes during lithiation [16].

be overcome in volumetric capacity, which mainly results from its high density (2621 mAh cm^{-3} based on a density of 6.24 g cm^{-3}, compared with S 3416 mAh cm^{-3} and Se 3246 mAh cm^{-3}) [9–12]. Indeed, volumetric capacity is playing a more important role in practical application of batteries, resulting from the limited space in portable electronics [10, 13]. Considering the aforementioned, Te can serve as a high-performance electrode material in modern energy storage systems due to its high volumetric capacity and high electronic conductivity [14, 15].

It can be attributed to the different molecular arrangement of S, Se, and Te. S crystal is constructed by S8 rings. Se crystals contain either Se8 rings or Se chains. However, Te crystal only has chain-like structures, which shows infinite helix structure (**Figure 2**) [17]. There are huge difference makes a fundamental effect on poly-sulfides, poly-selenides, and poly-tellurides. At the second step of dis-charge process, poly-tellurides are continuously reduced to the insoluble metal di-tellurides and/or tellurides (M2Te2 or M2Te, M: Li, Na, or K) [18, 19]. Interestingly, this mechanism is only applicable to alkali metal-Te batteries; Al-Te batteries are working based on a different mechanism, which will be discussed later. The basic reaction mechanism of Te can be described as follows: during discharge, the Te positive electrode is first reduced to chain-like poly-tellurides and cyclo poly-tellurides (M2[Ten]2−, 2 < n ≤ 8, M: Li, Na, K) at the first step, which is different from metal-S and metal-Se batteries (only chain-like poly-sulfides or poly-selenides are generated) [11].

2. Experimental

The Sn and Pb doped Tl$_{10-x}$A$_x$Te$_6$(A = Sn &Pb) is (x = 1.00, 1.25, 1.50, 1.75, 2.00) has been prepared by solid state reactions in evacuated sealed silica tubes. The purpose of this study were mainly for discovering new type of ternary and quaternary

compounds by using Tl^{+1}, Sn^{+3} and Te^{-2} elements as the starting materials. Direct synthesis of stoichiometric amount of high purity elements i.e. 99.99% of different compositions have been prepared for a preliminary investigation. Since most of these starting materials for solid state reactions are sensitive to oxygen and moistures, they were weighing stoichiometric reactants and transferring to the silica tubes in the glove box which is filled with Argon. Then, all constituents were sealed in a quartz tube. Before putting these samples in the resistance furnace for the heating, the silica tubes was put in vacuum line to evacuate the argon and then sealed it. This sealed power were heated upto 650 C^o at a rate not exceeding 1 k/mint and kept at that temperature for 24 hours. The sample was cooled down with extremely slow rate to avoid quenching, dislocations, and crystals deformation.
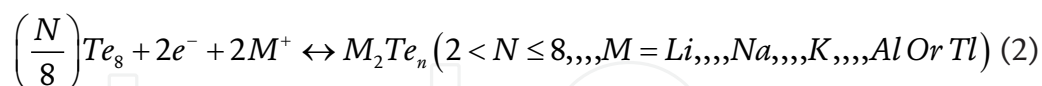
Structural analysis of all these samples was carried out by x-rays diffraction, using an Inel powder diffractometer with position-sensitive detector and CuKα radiation at room temperature. No additional peaks were detected in any of the sample discussed here. X-ray powder diffraction patterns confirm the single phase composition of the compounds.

The temperature dependence of Seebeck co-efficient was measured for all these compounds on a cold pressed pellet in rectangular shape, of approximately 5x1x1 mm^3 dimensions. The air sensitivity of these samples was checked (for one sample) by measuring the thermoelectric power and confirmed that these samples are not sensitive to air. This sample exposes to air more than a week, but no appreciable changes observed in the Seebeck values. The pellet for these measurements was annealed at 400 C^0 for 6 hours.
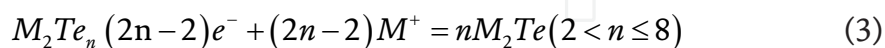
For the electrical transport measurements 4-probe resistivity technique was used and the pellets were cut into rectangular shape with approximate dimension of 5x1x1 mm^3. The proposed reaction equations are listed as follows.
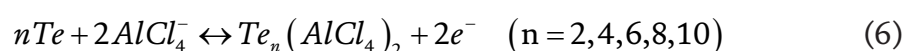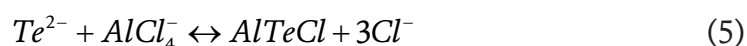
3. Chemical reactions

First step:

$$\left(\frac{N}{8}\right)Te_8 + 2e^- + 2M^+ \leftrightarrow M_2Te_n \left(2 < N \leq 8,,,,M = Li,,,,Na,,,,K,,,,Al\ Or\ Tl\right) \quad (2)$$

Second step:

$$M_2Te_n \left(2n-2\right)e^- + \left(2n-2\right)M^+ = nM_2Te \left(2 < n \leq 8\right) \quad (3)$$

Example.
Al-Te Battries:
Positive Electrode:

$$Te + 2e^+ \leftrightarrow Te^{2-} \quad (4)$$

$$Te^{2-} + AlCl_4^- \leftrightarrow AlTeCl + 3Cl^- \quad (5)$$

$$nTe + 2AlCl_4^- \leftrightarrow Te_n \left(AlCl_4\right)_2 + 2e^- \quad (n = 2,4,6,8,10) \quad (6)$$

$$Te_n\left(AlCl_4\right)_2 + \left(7n-2\right)AlCl_4^- \leftrightarrow nTeCl_3.AlCl_4 + 3nAl_2Cl_7 + \left(4n-2\right)e^- \quad (7)$$

Negative Electrode:

$$4\,Al_2Cl_7^- + 3e^- \leftrightarrow 7\,AlCl_4^- + Al \quad (8)$$

Overall Reaction:

$$5\,Al_2Cl_7^- + Te^{2-} \leftrightarrow 2\,Al + 7\,AlCl_4^- + TeCl_3.AlCl_4^- \quad (9)$$
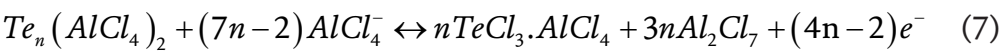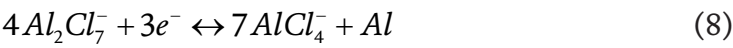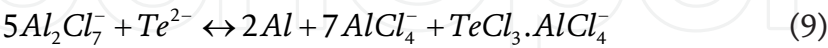
4. Result and discussions

4.1 Structural analysis

X-ray diffraction is used for the structural analysis of the materials. It helps to determine the crystal structure and particle size. Several of $Tl_{10-x}XTe_6$ which have doped Pb and Sn in it. The X is the different doped element. Where X is Pb and Sn. It has the different concentration of it. The X-ray diffraction of $Tl_{10-x}XTe_6$ with different concentration of doping of Pb and Sn as in **Figure 1**. Due to the different concentration, their peaks are different shown in **Figure 1**.

The **Figure 2** shows the EDX of the $Tl_{10-x}XTe_6$, have the different concentration of the doping of the Pb and Sn in it. The EDX shows the composition of the compounds. It shows the Pb and Sn are present in it.

4.2 Physical properties

To determine the different concentration of the doping of the Pb and Sn in the compound, there is changing in the charges carries. So the doping is effect on the temperature. Due to this temperature, it is variant in the Seebeck coefficient (S) as shown in **Figure 3**. The Seebeck coefficient can determined the temperature gradient for 1 K. It shows that the positive Seebeck effect from the 300 K to 500 K, for all p type semiconductors whose have the high charge carrier concentration. The Seebeck is positive due the concentration of doping elements is increase. So
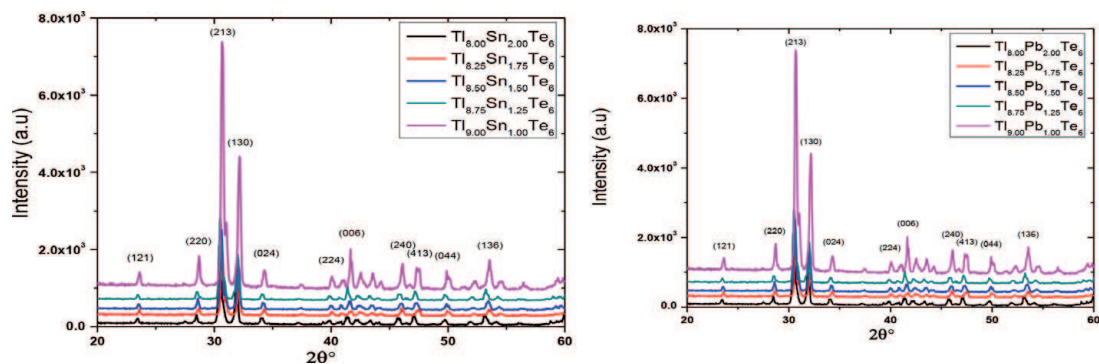

Figure 3.
XRD of doping of Sn and Pb in the TlXTe (X = Sn,Pb).

the mostly thermoelectric materials are the p type semiconductors materials. Due to increasing the concentration of doping elements, It improves the (i) reducing of grain size (ii) charge mobility and carrier density in thermos electric materials.

The Seebeck coefficient is varying from 80 to 120 μV/K as a function of the temperature. The behavior of the Seebeck coefficient is increasing as the Fermi level energy is decreasing due to the charge carrying density. In **Figure 4** shows that there is low level of charge carrier so that the holes are increase in it, so that it shows the high value of thermopower. So the large value of X, the doping elements have the large number of electrons and less number of charges carriers.

In **Figure 4** shows, the electrical conductivity of the quaternary compounds as compared to the temperature while the temperature is varied. The electrical conductivity is decrease as the temperature is increase that's why it is show the p type semiconductor and behave the positive temperature coefficient. It is cause the phonons scattering the charge carriers and effects the grains boundary. As increase the doping of elements, the holes in the compounds are increase, which is cause the phonons scattering. In chalcogenide system, the different elements are doping in the compound has no effect on the electrical conductivity. The low electrical conductivity is due to the effect oxide as the impurity in the compounds.

The behavior of temperature is different for the different concentration of the compound. The relationship between the Seebeck, temperature and concentration of doping elements as given below.

$$S = \frac{8\pi^2 k_B^2}{3eh^2} m^* T \left(\frac{\pi}{3n} \right)^{\frac{2}{3}} \tag{10}$$

Where, k_B is the Boltzmann constant, e is the electronic charge, h is the Planck's constant, m^* is the effective mass and n is the charge carrier concentration. The effective mass and concentration are two parameters of the Seebeck coefficient. The samples have low concentration, it increase the thermos-power as well as the temperature.

The **Figure 4** shows that the electrical conductivity σ is decrease as the increase of the temperature of the compounds. The Seebeck is inversely effect due to the increasing of the doping of the concentration of the doping.
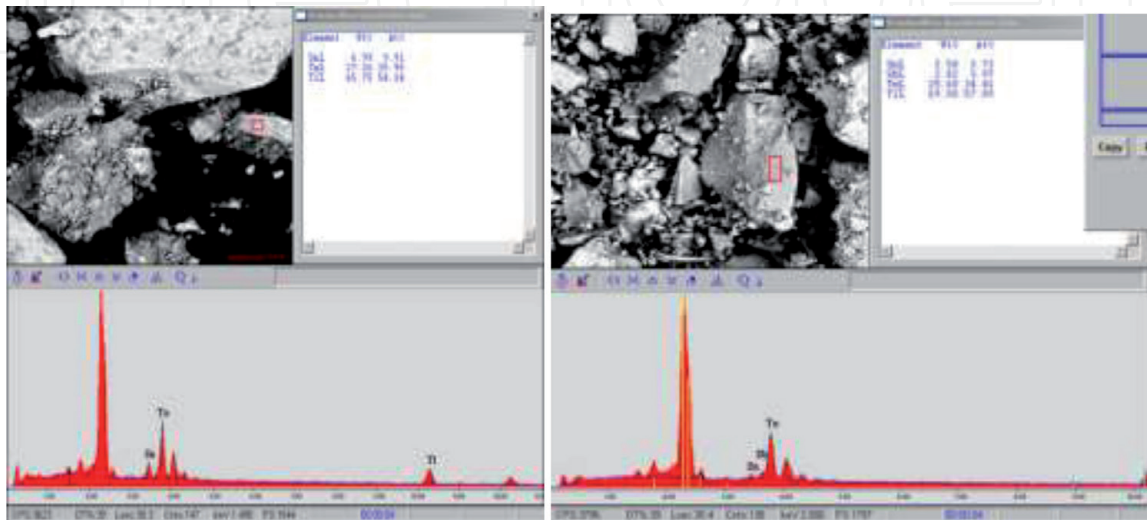

Figure 4.
Comparison of the EDX of doping of Pb and Sn in the TlXTe (X = Sn,Pb).

The different compounds have enhance the power factor (PF = $S^2 \sigma$) is decreases the electrical conductivity as increases the Seebeck coefficient in the given system. The PF is depend on the Seebeck coefficient. To measure the PF by the knowing the electrical conductivity and Seebeck coefficient in the **Figure 5**. As increases the temperature, the power factor is increases for all the compounds. In the **Figure 6** shows that the electrical conductivity is decreases as the increases the temperature is increases due the thermal vibration in compounds. The **Figure 7** shows that the power factor increase as the doping of the concentration is increases. As increases, the doping of the elements in the compounds is increase the optimization, which can help to increases the Seebeck and power factor (**Figures 5** and **7**).

Activity series of common metals

|		
Li		**Very active metals**
K		**K and Na react violently with water**
Ba		**They also react violently with acids.**
Sr		
Ca		
Na		
Mg		
Al		**Metals of intermediate activity.**
Mn		**React with steam or with acids such as HCl with liberation of H2**
Zn		
Cr		
Fe		
Cd		
Co		**Moderately active metals.**
Ni		**Do not react with water.**
Sn		**React slowly with the HCl.**
Pb		
H2		
Cu		**Moderately noble metals.**
Ag		**Do not react with water, HCl.**
Hg		
Pt		**Very noble metals.**
Au		**React only with Aqua Regia.**
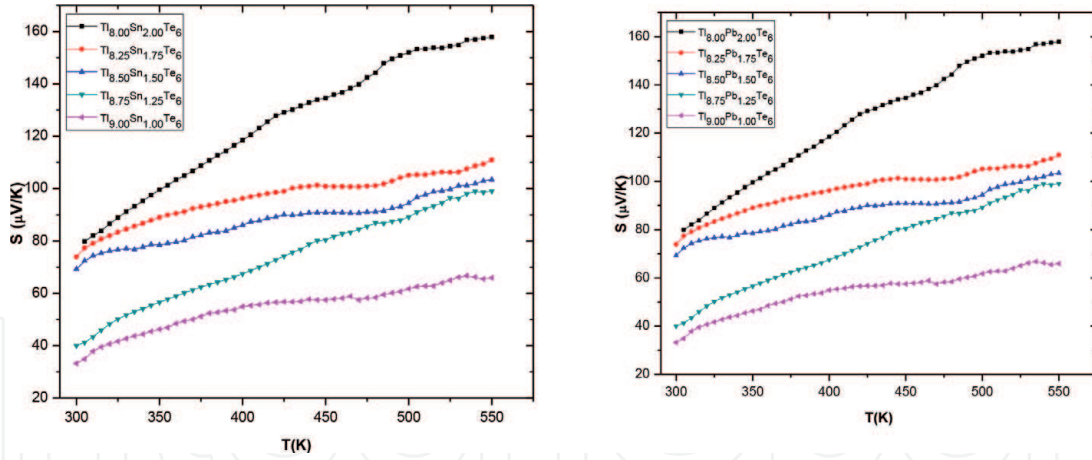
Figure 5.
Comparison of the see-beck coefficient of doping of Pb and Sn in the TlXTe (X = Sn,Pb).
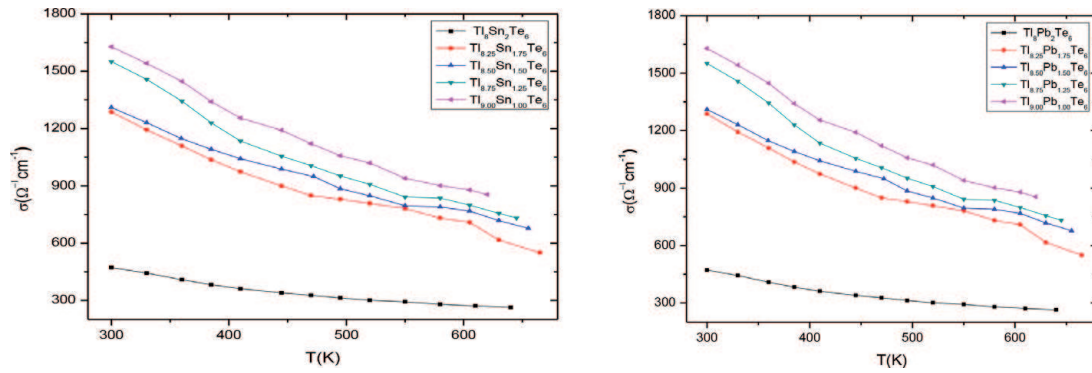

Figure 6.
Comparison of the electrical conductivity of doping of Pb and Sn in the TlXTe (X = Sn,Pb).
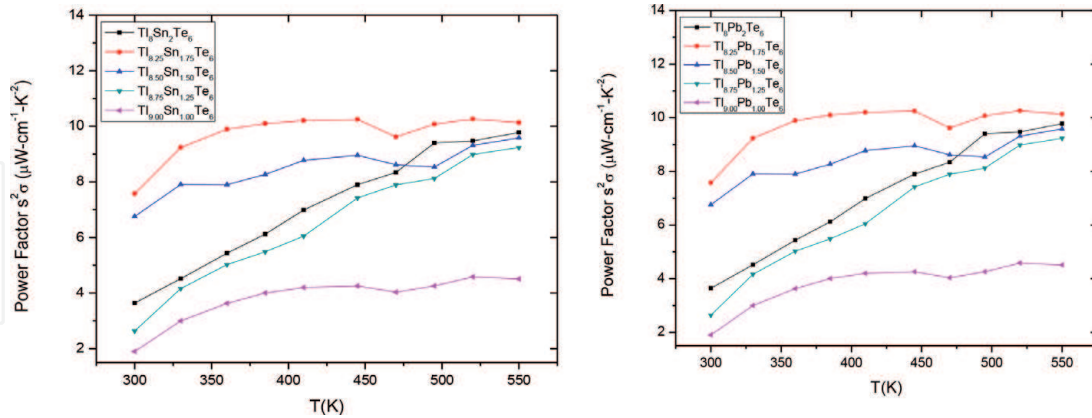

Figure 7.
Comparison of the power factor of doping of Pb and Sn in the TlXTe (X = Sn,Pb).

5. Conclusion

The different concentration of the doped Sn and Pb in the $Tl_{10-x}XTe_6$, is synthesized and then studied the physical properties. The XRD shows the compounds is the single phase, crystal structure measured by the experimental formula, having the same space group 14/mcm like Tl_5Te_3. The doping of the holes materials it changes its physical properties i.e. thermal, electrical, phase etc. Due the doping of Pb and Sn, the Seebeck coefficient is increases. The phase of the both compound

is also change. The phase is come to the face centered cubic.it is also shows that the increases temperature decreases the electrical conductivity. The power factor is increases because the Seebeck coefficient is increase.

Author details

Waqas Muhammad Khan* and Wiqar Hussain Shah
Department of Physics, Faculty of Basic and Applied Science, International Islamic University, Islamabad, Pakistan

*Address all correspondence to: waqaskhanrwp@gmail.com

IntechOpen

References

[1] T. Caillat, J. Fleurial, A. Borshchevsky, AIP conf. Proc. **420**, 1647 (1998).

[2] R.J. Campana, Adv. Ener. Conv. **2**, 303 (1962).

[3] R.J. Mehta, Y Zhang, C. Karthika eta, Nature Materials, **11**, 233-240 (2012).

[4] G.S. Nolas, J. Poon and M. Kanatzidis, MRS, Bull **31**199 (2006),

[5] B.A. Kuropaatawa, A. Assoud, H. Klienke, J. Alloys and Compounds **509**, 6768 (2011).

[6] K. Kurosaki, A. Kosuge, H. Muta, M. Uno, and S. Yamanaka, Applied Phys. Letts. **87**, 061919 (2005); J. Yang, F.R. Stablers, J. Electrn.Mater.**38**, 1245 (2009).

[7] G.J. Synder, E.S. Toberer, Nat. Mater. **7**, 105 (2008).

[8] J.R. Soostsman, D.Y. Chung, Kanatzdis, M.G. Angew Chem. Inter. Ed. **48**, 8616 (2009).

[9] R. Fang, S. Zhao, Z. Sun, D.-W. Wang, H.-M. Cheng, F. Li, Adv. Mater. 2017, **29**, 1606823.

[10] A. Eftekhari, *Sustain.* Energy Fuels 2017, **1**, 14.

[11] J. R. He, Y. F. Chen, W. Q. Lv, K. C. Wen, Z. G. Wang, W. L. Zhang, Y. R. Li, W. Qin, W. D. He, ACS Nano 2016, **10**, 8837.

[12] H. D. Jiao, D. H. Tian, S. J. Li, C. P. Fu, S. Q. Jiao, ACS Appl. Energy Mater. 2018, **1**, 4924.

[13] Y. Liu, J. W. Wang, Y. H. Xu, Y. J. Zhu, D. Bigio, C. S. Wang, J. Mater. Chem. A 2014, **2**, 12201.

[14] N. Ding, S.-F. Chen, D.-S. Geng, S.-W. Chien, T. An, T. S. A. Hor, Z.-L. Liu, S.-H. Yu, Y. Zong, Adv. Energy Mater. 2015, **5**, 1401999.

[15] S. Ullah, G. Yasin, A. Ahmad, L. Qin, Q. Yuan, A. U. Khan, U. A. Khan, A. U. Rahman, Y. Slimani, Inorg. Chem. Front. 2020, **7**, 1750.

[16] Y. Wang, H.-L. Fei, Ionics 2013, **19**, 771.

[17] J. R. He, W. Q. Lv, Y. F. Chen, K. C. Wen, C. Xu, W. L. Zhang, Y. R. Li, W. Qin, W. D. He, ACS Nano 2017, **11**, 8144.

[18] H. M. Li, K. L. Wang, H. Zhou, X. L. Guo, S. J. Cheng, K. Jiang, *Energy Storage* Mater. 2018, **14**, 267.

[19] S. Lee, H. Choi, K. Eom, J. Power Sources 2019, **430**, 112.